Thin Solid Films 519 (2011) 5634–5637

Contents lists available at ScienceDirect

Thin Solid Films

journal homepage: www.elsevier.com/locate/tsf

Enhanced efficiency in mixed host red electrophosphorescence devices

Zisheng Su, Wenlian Li *, Bei Chu *

Key Laboratory of Excited State Processes, Changchun Institute of Optics, Fine Mechanics and Physics, Chinese Academy of Sciences, Changchun 130033, People's Republic of China

ARTICLE INFO

Article history:
Received 23 May 2010
Received in revised form 1 March 2011
Accepted 1 March 2011
Available online 13 March 2011

Keywords:
Organic light-emitting device
Mixed host
Electrophosphorescence

ABSTRACT

Enhanced efficiency of red phosphorescent organic light-emitting devices is observed by using a bis[2-(2′-benzothienyl)pyridinato-N,C$^{3'}$] iridium(acetylacetonato) doped 4,4′-N,N′-dicarbazole-biphenyl (CBP) and 1,3,5-tris(N-phenylbenzimidazole-2-yl)benzene (TPBI) mixed host emitting layer. The CBP:TPBI mixed host device shows a maximum external quantum efficiency of 9.1%, which is dramatically improved compared to that of the CBP (6.6%) and TPBI (5.4%) single host devices. Such a mixed host strategy can also be exploited in red phosphor dibenzo[*f*,*h*]quinoxaline iridium (acetylacetonate) doped devices. Investigations reveal that the position of charge carrier recombination zone of the mixed host devices predominantly locates in the electron blocking layer/emitting layer interface. The efficiency enhancement is attributed to the optimized hole and electron injection balance and hence increased charge carrier recombination rate in the emitting layer.

1. Introduction

Phosphorescent organic light-emitting devices (PHOLEDs) have attracted a great deal of interest because they can harvest both the singlet and triplet excitons, leading to a maximum internal quantum efficiency of 100% as compared with its fluorescent counterparts that only a maximum of 25% can be theoretically obtained [1]. Since the first demonstration of the PHOLEDs [2], much effort has been paid to improve their performance and a major breakthrough has been obtained. A maximum external quantum efficiency (η_{ext}) of nearly 20% has been realized in green and blue PHOLEDs [3–8]. However, the development of high efficient red PHOLED lags far behind that of the green and blue ones. For flat panel display and solid-state lighting, high efficient red PHOLED is desired and many methods have been proposed to improve their performance [9–13].

The electron–hole charge-balance factor plays an important role in determining the performance of the organic light-emitting devices (OLEDs). A mixed host strategy has often been used in fluorescent OLEDs to improve the efficiency, operating lifetime, and to decrease driving voltage [14–16]. Recently, such a mixed host strategy has been developed in green and blue PHOLEDs, and dramatically improved electroluminescent (EL) performance has been demonstrated [17–20]. The improvement was attributed to the more balanced charge carriers density and extended charge carriers recombination zone in the emitting layers (EMLs). The narrow band gap of the red phosphorescent emitters compared to the green and blue ones plays a crucial role on the charge carrier transport in their doped EMLs. It is thus of interest to see whether such a mixed host structure can be exploited in red PHOLEDs. In this letter, dramatically enhanced efficiency in red PHOLEDs is demonstrated by using the 4,4′-N,N′-dicarbazole-biphenyl (CBP) and 1,3,5-tris(N-phenylbenzimidazole-2-yl)benzene (TPBI) mixed host structure, and the improved performance is attributed to the balanced hole and electron injection and hence increased charge carrier recombination rate in the EMLs.

2. Experimental

Devices were fabricated on pattered indium tin oxide (ITO) coated glass substrates with a sheet resistance of 25 Ω/sq. The substrates were routinely cleaned and treated in an ultraviolet-ozone environment for 10 min before loading into a high vacuum chamber. Organic layers and the cathode were deposited onto the substrates via thermal evaporation. The devices have the structure of ITO/4,4′,4″-tris[2-naphthyl(phenyl)amino]-triphenylamine (2-TNATA, 10 nm)/N,N′-diphenyl-N,N′-bis(1-naphthyl)-(1,1′-benzidine)-4,4′-diamine (NPB, 20 nm)/4,4′,4″-tris(N-carbazolyl)triphenylamine (TCTA, 10 nm)/EML (30 nm)/TPBI (30 nm)/LiF (0.5 nm)/Al (100 nm). The host in the EML consisted of CBP mixed with different weight ratio of TPBI (0, 25%, 50%, 75%, and 100%, Devices A–E, respectively). A typical red phosphor bis[2-(2′-benzothienyl)pyridinato-N,C$^{3'}$] iridium(acetylacetonato) [btp$_2$Ir(acac)] with a phosphorescence quantum yield of 0.21 in solution [21] was selected as the dopant, and the doping concentration of all devices was fixed at 8 wt.%. The molecular structure of btp$_2$Ir(acac) is shown in the inset of Fig. 1. All the materials were brought from Nichem (Taiwan) except btp$_2$Ir(acac), and the materials were used as received without further purification. Btp$_2$Ir(acac) was synthesized in our laboratory with the method as reported by Lamansky et al. [21] and purified by the method of recrytallization before using. Deposition rates and thickness of the layers were monitored in situ using oscillating quartz monitors. The evaporating rates were kept at 0.5–1 Å/s for organic layers and LiF

* Corresponding authors. Tel./fax: +86 431 86176345.
E-mail addresses: wllioel@yahoo.com.cn (W. Li), beichu@163.com (B. Chu).

0040-6090/$ – see front matter © 2011 Elsevier B.V. All rights reserved.
doi:10.1016/j.tsf.2011.03.008

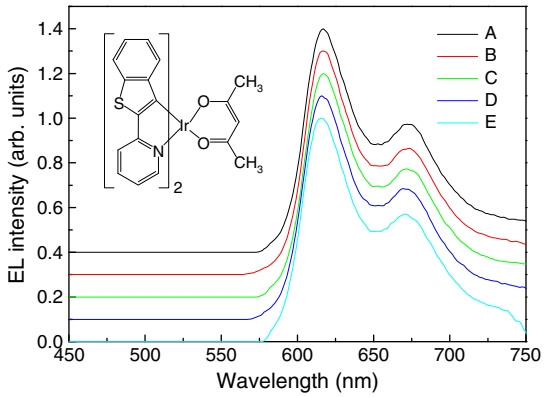

Fig. 1. EL specta of Devices A-E at applied of 10 V. Inset: molecular structure of $btp_2Ir(acac)$.

layer, and 10 Å/s for Al cathode, respectively. EL spectra and CIE coordinates of the devices were measured with an Opt-2000 CCD spectrometer (Optpe, China), which is connected to a computer and controlled by a program. Luminance–current–voltage (L-I-V) characteristics were measured with a Keithley 2400 power supply combined with a calibrated Si photodiode and were recorded simultaneously with measurements. η_{ext} of the PHOLEDs was calculated from their EL spectra and L-I-V characteristics under the assumptions that the emission pattern is Lambertian and the EL spectra are angle independent [22]. All the measurements were carried out at room temperature under ambient conditions.

3. Results and discussions

Fig. 1 shows the EL spectra of Devices A–E at applied bias of 10 V. It can be found that the devices have almost the same EL spectra with an emission peak at about 617 nm and a shoulder at about 672 nm, which are the characteristics of the emission of $btp_2Ir(acac)$. The CIE coordinates are (0.68, 0.32) and the EL spectra do not change with the applied voltage (not shown here). The same shape of EL spectra of the devices indicates that the addition of TPBI as the host matrix codopant has no influence on the emission spectrum of $btp_2Ir(acac)$.

The L-I-V characteristics of Devices A, C, and E are provided in Fig. 2. Among the three devices, Devices E and A have the highest and lowest current density at the same applied voltage, respectively. Such a fact suggests that the electron mobility in the $btp_2Ir(acac)$ doped EML plays a more important role in determining the device current density. The lower current density of Device A should be ascribed to the low electron mobility of the $btp_2Ir(acac)$ doped CBP layer. The turn on voltage of Devices A, C, and E are 4.5, 3.6, and 3.5 V, respectively. The lower turn on voltage of Devices C and E indicates that the addition of TPBI as host matrix codopant improves the electron mobility of the EMLs, which will be discussed latter.

Fig. 3 illustrates the η_{ext} as a function of current density for Devices A–E. The maximum η_{ext} of the CBP single host device (Device A) and the TPBI single host device (Device E) are 6.6% and 5.4%, respectively. The efficiency increases with the content of TPBI in the mixed host devices, and a maximum η_{ext} of 9.1% is obtained in the CBP:TPBI (50:50) mixed host device (Device C). Then the efficiency decreases with further increase of TPBI, as listed in Table 1. The maximum η_{ext} of Device C is enhanced about 40% and 70% compared to that of Devices A and E, respectively. Accompanying with the enhanced efficiency, an increased *efficiency roll-off* of the mixed host devices is found. The η_{ext} of Devices A, C, and E at 100 mA/cm^2 are 3.3%, 3.2%, and 1.7%, suggesting a roll-off of 50%, 65%, and 69% to their maximum, respectively. Although Device C shows more significant efficiency roll-off than that of Device A, the efficiency of Device C at high current density is comparable to Device A and higher than that of Device E. Similar enhancements of the *luminous* efficiency and power efficiency are found in the mixed host devices, and the maximum *luminous efficiency* and power efficiency of Device C are 7.9 cd/A and 5.4 lm/W, respectively, as listed in Table 1.

Fig. 4 depicts the η_{ext} versus luminance curves for Devices A–E. The η_{ext} of Devices A, C, and E at 100 cd/m^2 are 6.5%, 8.8%, and 5.3%, and they decreases to 3.8%, 4.0%, and 1.3% at 2000 cd/m^2, respectively. It is noted that although the efficiency of the mixed host devices is dramatically increased, they are still lower than that of same state-of-the-art red PHOLEDs reported [10–12].

In order to obtain high efficient red PHOLEDs, red phosphors with higher quantum yield should be used. To show that the efficiency enhancement is not specific to only $btp_2Ir(acac)$ doped mixed host devices, dibenzo[*f*,*h*]quinoxaline iridium (acetylacetonate) [$Ir(DBQ)_2(acac)$] with a phosphorescence quantum yield of 0.53 in solution [23] is adopted as the red emitter, the molecular structure of $Ir(DBQ)_2(acac)$ is shown in the inset of Fig. 5. $Ir(DBQ)_2(acac)$ was synthesized in our laboratory with the method as reported by Duan et al. [23] and purified by the method of recrytallization before using. Three devices with a structure similar to Devices A, B, and C but with $Ir(DBQ)_2(acac)$ as dopant were fabricated, respectively (hereafter denoted as A2, B2, and C2, respectively). Fig. 5 compiles the EL spectra of Devices A2–C2 at applied bias of 10 V. The three devices present almost the same EL spectra with an emission peak at about 613 nm and CIE coordinates of (0.62, 0.38), which is attributed to the emission of $Ir(DBQ)_2(acac)$.

The η_{ext} as a function of current density for Devices A2, B2, and C2 are presented in Fig. 6. Device A2 shows a maximum η_{ext} of 6.9%, corresponding to a maximum luminous efficiency and power efficiency of 10.2 cd/A and 6.1 lm/W, while the maximum η_{ext} of Device C2 is 9.6%, corresponding to a maximum luminous efficiency and power efficiency of 14.3 cd/A and 9.2 lm/W, respectively. The

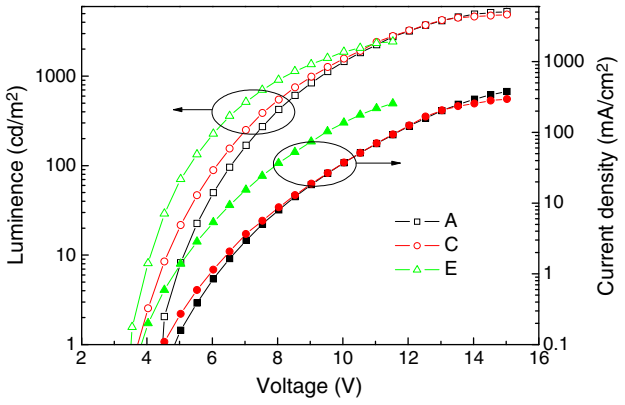

Fig. 2. L-I-V characteristics of Devices A, C, and E.

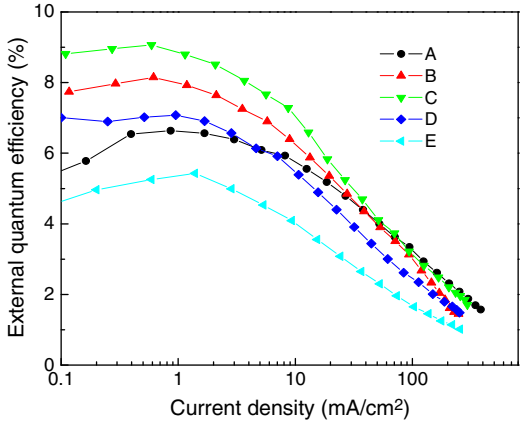

Fig. 3. η_{ext} as a function of current density for Devices A–E.

Table 1
Maximum η_{ext}, *luminous efficiency* (η_c), and power efficiency (η_p) of Devices A–E.

Device	Max η_{ext} (%)	Max η_c (cd/A)	Max (lm/W)
A	6.6	5.8	3.2
B	8.2	7.3	4.8
C	9.1	7.9	5.4
D	7.1	6.4	4.4
E	5.4	5.1	3.5

lower efficiencies of Device A2 compared to that reported by Duan et. al [23] should be ascribed to the different device structure and/or low material purity of Ir(DBQ)$_2$(acac). It is interesting to find that the efficiency of the mixed host devices is higher than the reference Device A2 in the whole current density region. The η_{ext} of Devices A2, B2, and C2 at 100 mA/cm^2 are 3.8%, 4.4%, and 4.9%, respectively. The fact that the enhancement of η_{ext} is found in both btp$_2$Ir(acac) and Ir(DBQ)$_2$(acac) based mixed host PHOLEDs suggests that such a mixed host structure may has the potential application in increasing the efficiency of the other red PHOLEDs.

Fig. 7 illustrates the schematic energy diagram of the devices. The values of the highest occupied molecular orbital (HOMO) and lowest unoccupied molecular orbital (LUMO) of the materials were cited from the literature [13,20,24]. TPBI is an electron transporting material with a high electron mobility. The HOMO and LUMO of TPBI are 6.2 and 2.4 eV, respectively. The lower HOMO of TPBI compared to TCTA forms a large injection barrier for holes and consequently the position of charge carrier recombination zone is expected to locate in a very narrow region in the EML near to TCTA/EML interface when TPBI is adopted as the host material for the red PHOLEDs [3,13]. The narrow recombination zone would lead to a narrow light emitting region and hence high exciton density in this region at high current density, which results in serious triplet–triplet annihilation and triplet–polaron annihilation and hence significant efficiency roll-off [25,26], as shown in Fig. 3.

To determine the position of charge carrier recombination zone of Devices A and C, a 1 nm rubrene sensing layer was inserted to the EMLs at the positions with the distance of 0, 10, 20, and 30 nm away from the TCTA/EML interface, respectively. The singlet and triplet energies of rubrene are 2.2 and 1.2 eV [27], while the singlet and triplet energies of btp$_2$Ir(acac) are 2.7 and 2.0 eV [28], respectively. Thus the energy transfers from btp$_2$Ir(acac) singlet to rubrene singlet and from btp$_2$Ir(acac) triplet to rubrene triplet are energetically favorable. However, due to the high intersystem crossing efficiency from btp$_2$Ir(acac) singlet to triplet, the energy transfer from btp$_2$Ir(acac) singlet to rubrene singlet can be neglected. Although the singlet energy of rubrene is higher than the triplet energy of btp$_2$Ir(acac), the energy transfer from rubrene singlet to btp$_2$Ir(acac) triplet

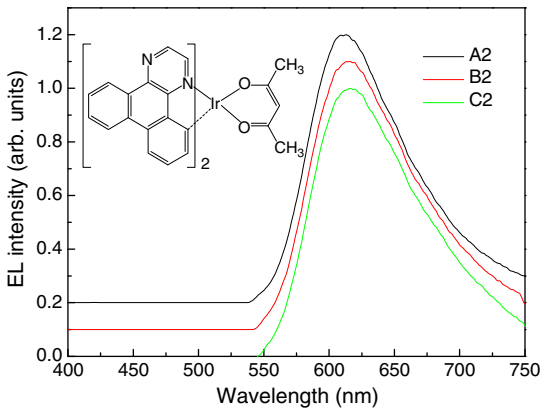

Fig. 5. EL spectra of Devices A2–C2 at applied bias of 10 V. Inset: molecular structure of Ir(DBQ)$_2$(acac).

is a spin forbidden transition and is not allowed. Thus the only possible energy transfer process is from btp$_2$Ir(acac) triplet to rubrene triplet. When the rubrene molecules are closed to the btp$_2$Ir(acac) molecules, the emission intensity of btp$_2$Ir(acac) which comes from the transition of triplet excitons would decrease due to the energy transfer from btp$_2$Ir(acac) triplet to rubrene triplet, while the emission intensity of rubrene which comes from the transition of singlet excitons would be unaffected. Exciton formation probability is in proportion to the product of the electron and hole densities [29]. Both the rubrene emission intensity and the btp$_2$Ir(acac) triplet to rubrene triplet energy transfer efficiency are in proportion to the exciton formation probability in the region where the rubrene sensing layer were inserted. Given that the insert of the thin rubrene layer has no effect on the charge carriers transport properties and consequently the poison of the charge carrier recombination zoon. Then the poison of the charge carrier recombination zoon can be simply determined by the relative emission intensity of rubrene/btp$_2$Ir(acac), and it would locate predominant in the region where it has the highest relative emission intensity of rubrene/btp$_2$Ir(acac). Fig. 8 shows the relative emission intensity of rubrene/btp$_2$Ir(acac) at 560 and 617 nm, respectively, with different sensing layer position in Devices A and C at current density of 20 and 200 mA/cm^2. As can be found in the figure, the position of charge carrier recombination zone of Device A predominantly locates at EML/TPBI and TCTA/EML interfaces at low driving current, and no distinct shift of charge carrier recombination zone with current density is observed, indicating that the position of charge carrier recombination zone is almost current independent in Device A. While the position of charge recombination zone of Device C

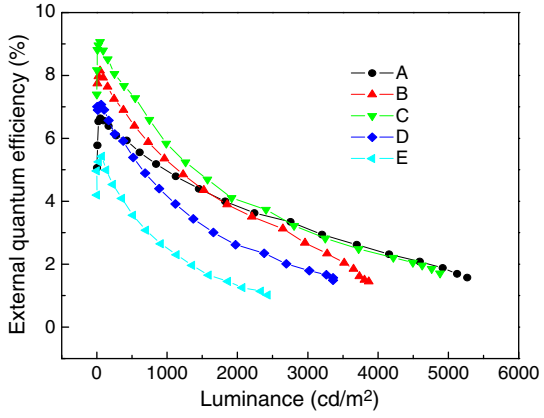

Fig. 4. η_{ext} versus luminance curves of Devices A–E.

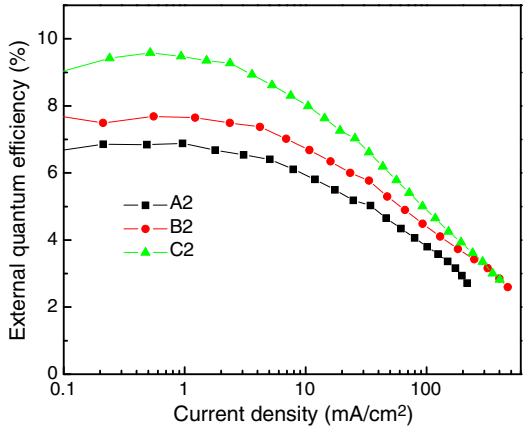

Fig. 6. η_{ext} as a function of current density for Ir(DBQ)$_2$(acac) doped Devices A2–C2.

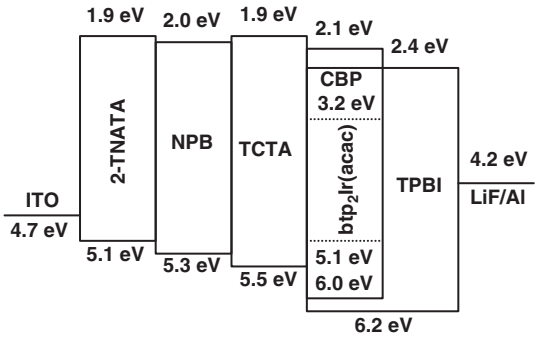

Fig. 7. Schematic energy diagram of the PHOLEDs.

predominantly locates at the TCTA/EML interface at low driving current and it extends to the whole EML at high current density.

The HOMO and LUMO of CBP are 6.0 and 2.1 eV, while they are 5.1 and 3.2 eV for $btp_2Ir(acac)$, respectively. The large HOMO and LUMO offsets between CBP and $btp_2Ir(acac)$ would form deep traps for hole and electron transporting in the CBP:$btp_2Ir(acac)$ EML, respectively. Consequently, holes and electrons will accumulate in the TCTA/EML and EML/TPBI interfaces in Device A, respectively. On the other hand, the hole and electron blocking properties of TPBI and TCTA would confine the holes and electrons in the EML/TPBI and TCTA/EML interfaces, respectively. Thus the position of charge carrier recombination zone located in the TCTA/EML and EML/TPBi interfaces can be reasonable understood for Device A, as found in Fig. 8. When TPBI is adopted as the cohost in Device C, the lower LUMO of TPBI at 2.4 eV in comparison to CBP at 2.1 eV would reduce the electron injection barrier from the electron transporting layer TPBI to the EML and facilitate electron transporting to the TCTA/EML interface, while hole was further restricted to transport to the EML/TPBI interface. Such effects lead to the increased electron and hole densities and hence increased exciton formation probability in the TCTA/EML interface. Thus the position of charge recombination zone is expected to be predominantly located in the TCTA/EML interface in Device C at low current density, as found in Fig. 8. At high current density the number of hole that transporting into the bulk of the EML would increase, resulting in an extended charge recombination zone to the whole EML. Such a broadened charge carrier recombination zone is in favor of reducing the efficiency roll-off and increasing the device lifetime. It is noted that there is no apparently broadened charge recombination zone in Device C as refer to Device A at low current density, thus such a mechanism can be ruled out for the enhanced performance of the mixed host red PHOLEDs. The enhanced efficiency should be attributed to the optimized hole and electron injection balance and hence increased charge carrier recombination rate in the EML. Although the increased exciton density in the emitting region leads to more serious triplet–triplet annihilation and triplet–polaron annihilation and hence more pronounced efficiency roll-off, the efficiency of the mixed host red PHOLEDs can be higher than the single host devices even at high current density.

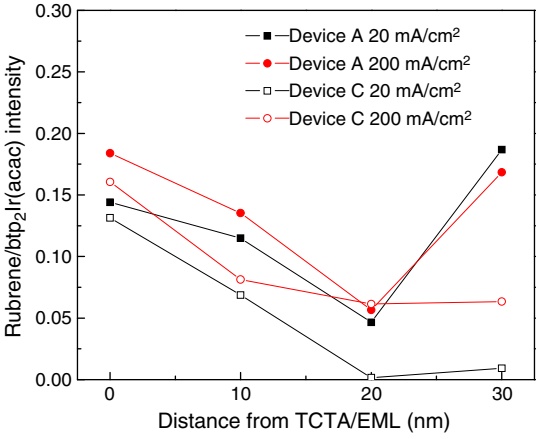

Fig. 8. Relative emission intensity of rubrene to $btp_2Ir(acac)$ when the rubrene sensing layer was embedded in different position in the EML of CBP single host and CBP:TPBI (50:50) mixed host devices.

4. Conclusions

In summary, a CBP:TPBI mixed host strategy is adopted in red phosphors $btp_2Ir(acac)$ doped PHOLEDs. The CBP:TPBI (50:50) mixed host device shows a maximum external quantum efficiency of 9.1%, which is dramatically improved compared to that of the CBP and TPBI single host devices. The position of charge carrier recombination zone of the mixed host devices predominantly locates in the electron blocking layer/EML interface, and it extends to the whole EML at high current density. The improved performance of the mixed host devices is attributed to the more balanced hole and electron injection and hence increased charge carrier recombination rate in the EML. Similar performance improvement is found in the Ir $(DBQ)_2(acac)$ doped red PHOLEDs, indicating that such a mixed host structure may has the potential application in increasing the efficiency of the red PHOLEDs.

Acknowledgments

This work was supported by the National Natural Science Foundation of China (grant nos. 60877027, 61076047, and 11004187) and by the Knowledge Innovation Project of Chinese Academy of Sciences (no. KJCX2-YW-M11).

References

[1] M.A. Baldo, D.F. O'Brien, M.E. Thompson, S.R. Forrest, Phys. Rev. Lett. 60 (1999) 14,422.
[2] M.A. Baldo, D.F. O'Brien, Y. You, A. Shoustikov, S. Sibley, M.E. Thompson, S.R. Forrest, Nat. Lond. 395 (1998) 151.
[3] C. Adachi, M.A. Baldo, M.E. Thompson, S.R. Forrest, J. Appl. Phys. 90 (2001) 5048.
[4] M. Ikai, S. Tokito, Y. Sakamoto, T. Suzuki, Y. Taga, Appl. Phys. Lett. 79 (2001) 156.
[5] S.O. Jeon, K.S. Yook, C.W. Joo, J.Y. Lee, K.Y. Ko, J.Y. Park, Y.G. Baek, Appl. Phys. Lett. 93 (2008) 063306.
[6] N. Chopra, J. Lee, Y. Zheng, S.H. Eom, J. Xue, F. So, Appl. Phys. Lett. 93 (2008) 143,307.
[7] H. Fukagawa, K. Watanabe, T. Tsuzuki, S. Tokito, Appl. Phys. Lett. 93 (2008) 133,312.
[8] S.O. Jeon, K.S. Yook, C.W. Joo, J.Y. Lee, Appl. Phys. Lett. 94 (2009) 013301.
[9] C. Adachi, M.A. Baldo, S.R. Forrest, S. Lamansky, M.E. Thompson, R.C. Kwong, Appl. Phys. Lett. 78 (2001) 1622.
[10] R. Meerheim, K. Walzer, M. Pfeiffer, K. Leo, Appl. Phys. Lett. 89 (2006) 061111.
[11] H. Kanno, K. Ishikawa, Y. Nishio, A. Endo, C. Adachi, K. Shibata, Appl. Phys. Lett. 90 (2007) 123,509.
[12] T. Tsuzuki, S. Tokito, Appl. Phys. Lett. 94 (2009) 033302.
[13] H. Baek, C. Lee, J. Appl. Phys. 103 (2008) 054510.
[14] H. Aziz, Z.D. Popovic, N.X. Hu, Appl. Phys. Lett. 81 (2002) 370.
[15] J.H. Lee, C.I. Wu, S.W. Liu, C.A. Huang, Y. Chang, Appl. Phys. Lett. 86 (2005) 103,506.
[16] Y.G. Lee, S.K. Kang, T.S. Oh, H.N. Lee, S. Lee, K.H. Koh, Org. Electron. 9 (2008) 339.
[17] M.E. Kondakova, J.C. Deaton, D.Y. Kondakov, T.D. Pawlik, R.H. Young, C.T. Brown, D.J. Giesen, SID Int. Symp. Dig. Tech. Pap. 38 (2007) 837.
[18] S.H. Kim, J. Jang, K.S. Yook, J.Y. Lee, Appl. Phys. Lett. 92 (2008) 023513.
[19] M.T. Lee, J.S. Lin, M.T. Chu, M.R. Tseng, Appl. Phys. Lett. 92 (2008) 173,305.
[20] M.E. Kondakova, T.D. Pawlik, R.H. Young, D.J. Giesen, D.Y. Kondakov, C.T. Brown, J.C. Deaton, J.R. Lenhard, K.P. Klubek, J. Appl. Phys. 104 (2008) 094501.
[21] S. Lamansky, P. Djurovich, D. Murphy, F. Abdel-Razzaq, H.E. Lee, C. Adachi, P.E. Burrows, S.R. Forrest, M.E. Thompson, J. Am. Chem. Soc. 123 (2001) 4303.
[22] H. Li, C. Zhang, D. Li, Y. Duan, J. Lumin. 122–123 (2007) 626.
[23] J.P. Duan, P.P. Sun, C.H. Cheng, Adv. Mater. Weinheim Ger. 15 (2003) 224.
[24] K. Okumoto, Y. Shirota, J. Lumin. 87–89 (2000) 1171.
[25] M.A. Baldo, C. Adachi, S.R. Forrest, Phys. Rev. B 62 (2000) 10,967.
[26] S. Reineke, K. Walzer, K. Leo, Phys. Rev. B 75 (2007) 125,328.
[27] T.N. Singh-Rachford, F.N. Castellano, J. Phys. Chem. A 112 (2008) 3550.
[28] C. Rost-Bietsch, Ambipolar and light-emitting organic field-effect transistors, Göttingen Cuvillier, 2005.
[29] Y. Sun, N.C. Giebink, H. Kanno, B. Ma, M.E. Thompson, S.R. Forrest, Nat. Lond. 440 (2006) 908.